Supporting Information

$VO_2 \cdot 0.26H_2O$ Nanobelts@Reduced Graphene Oxides as Cathode Materials for High-Performance Aqueous Zinc Ion Batteries

Ling Xie[a], Wenhai Xiao[a], Xiaoyan Shi[a], Junzhi Hong[a], Junjie Cai,[a] Kaili Zhang[b], Lianyi Shao[a,*], Zhipeng Sun[a,*]

[a]*School of Materials and Energy, Guangdong University of Technology, Guangzhou 510006, Guangdong, China, E-mail: shaolianyi@gdut.edu.cn (Lianyi Shao), zpsunxj@gdut.edu.cn (Zhipeng Sun).*

[b]*Department of Mechanical Engineering, City University of Hong Kong, 83 Tat Chee Avenue, Hong Kong, China*

Experimental section

1. Materials and methods

Graphene oxide (GO) required for the experiment was purchased directly from XFNANO company. A rapid and scalable microwave-assisted hydrothermal method was adopted for the synthesis of highly homogenous $VO_2 \cdot 0.26H_2O$@rGO. In a typical procedure, 3 mmol anhydrous oxalic acid was first dissolved in 26 mL of deionized water with stirring, 1.8 mmol NH_4VO_3 was then added and stirred for 2 hours at 60°C. Next, 4 mL of GO (5 mg/mL) and 10 mg of PVP were dispersed in the above solution and stirred at room temperature to form a homogeneous solution, and finally transferred to a Teflon-lined autoclave. The autoclave was then placed in a microwave-hydrothermal synthesis system. The system temperature was increased to 190°C within 15 minutes and maintained for 180 minutes. After the reaction, the resulting product was collected by filtration and washed with distilled water, and subsequent vacuum freeze dried. Pure $VO_2 \cdot 0.26H_2O$ was prepared by the same synthetic route without GO solution.

2. Material characterization

The crystallographic structure and phase purity of $VO_2 \cdot 0.26H_2O$ and $VO_2 \cdot 0.26H_2O$@rGO were identified by X-ray diffraction (XRD, Rigaku Smart Lab diffractometer) with Cu K αradiation. Raman spectroscopy was obtained on Lab RAM HR Evolution. Scanning electron microscopy (SEM, Hitachi SU8010) and transmission electron microscopy (TEM, FEI Thermo Talos F200S) were applied to obtain the morphologies and elemental mapping of active materials. Brunauer-Emmett-Teller (BET) surface area was obtained by nitrogen adsorption-desorption isotherms using BELSORP-Mini instrument. Thermogravimetric analysis (TG, Mettler, 3+/1600HT) of materials was carried out in nitrogen atmosphere and air at a temperature range of 50-600 °C with a heating rate of 10°C min^{-1}. Chemical components were acquired by X-ray photoelectron spectroscopy (XPS, Thermo Fisher ESCALAB 250Xi). The conductivity was measured by a digital 4-point probes resistivity measurement system (ST2253).

3. Electrochemical measurements

To make cathode for ZIBs, active materials, Super P and polyvinylidene fluoride were ground in a gravimetric ratio of 7:2:1 in n-methyl-2-pyrrolidone. This mixed slurry was deposited onto stainless steel mesh with a diameter of 12 mm and vacuum-dried at 60°C for 12 hours. The mass loading of active material on electrode was approximately 1.5-2 mg cm^{-2}. To test the electrochemical performance of cathode, 2032-type coin cells was assembled in air with pure zinc foil (100 um) as counter electrode, 3 M Zn $(CF_3SO_3)_2$ as electrolyte, and glass fiber as separator. Cyclic voltammetry (CV) profiles were acquired on electrochemical workstation (CHI 660E) in 0.2-1.3 V. The discharge/charge tests and galvanostatic intermittent titration technique (GITT) of samples were cycled using a battery testing system (NEWARE TECHNOLOGY IMITED, CT-4008) in 0.2-1.3 V. Electrochemical impedance spectroscopy (EIS) was collected by electrochemical workstation (CHI 660E) in the frequency range of 0.1-10^5 Hz.

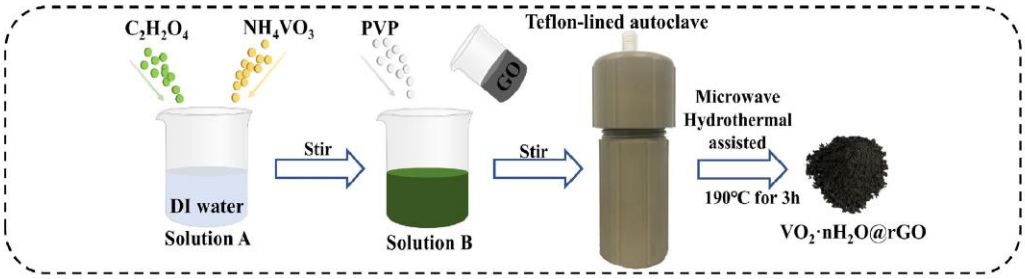

Fig. S1. Illustration of production process.

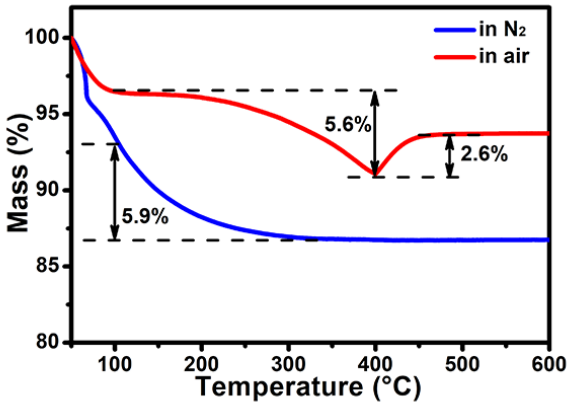

Fig. S2. TG curves for $VO_2 \cdot 0.26H_2O$.

For $VO_2 \cdot 0.26H_2O$, the weight loss can be ascribed to the vaporization of the physically absorbed water (50-100°C) and structural water (100-400°C).[1] In addition, it can be found that the weight of $VO_2 \cdot 0.26H_2O$ increases in the temperature range between 400 and 450°C in air, probably because VO_2 converts to V_2O_5.[2] On account of the reduced weight is 5.9% in the nitrogen atmosphere, the ratio of crystal water can be calculated as about 0.26 per mole.

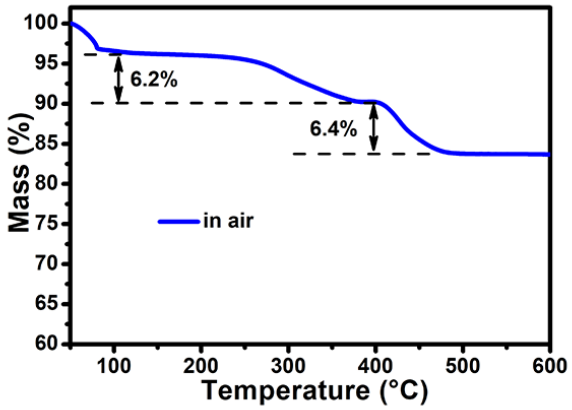

Fig. S3. TG curve for $VO_2 \cdot 0.26H_2O$@rGO in air.

For $VO_2 \cdot 0.26H_2O$@rGO, the weight loss also can be ascribed to the vaporization of the physically absorbed water (50-100°C) and structural water (100-400°C) in air. Especially, the mass loss of $VO_2 \cdot 0.26H_2O$@rGO in the range of 400-480°C in air is ascribed to the thermal decomposition of rGO carbon skeleton.[3] Thus, the mass fraction of rGO in the composite can estimated to be 12.3%.[4]

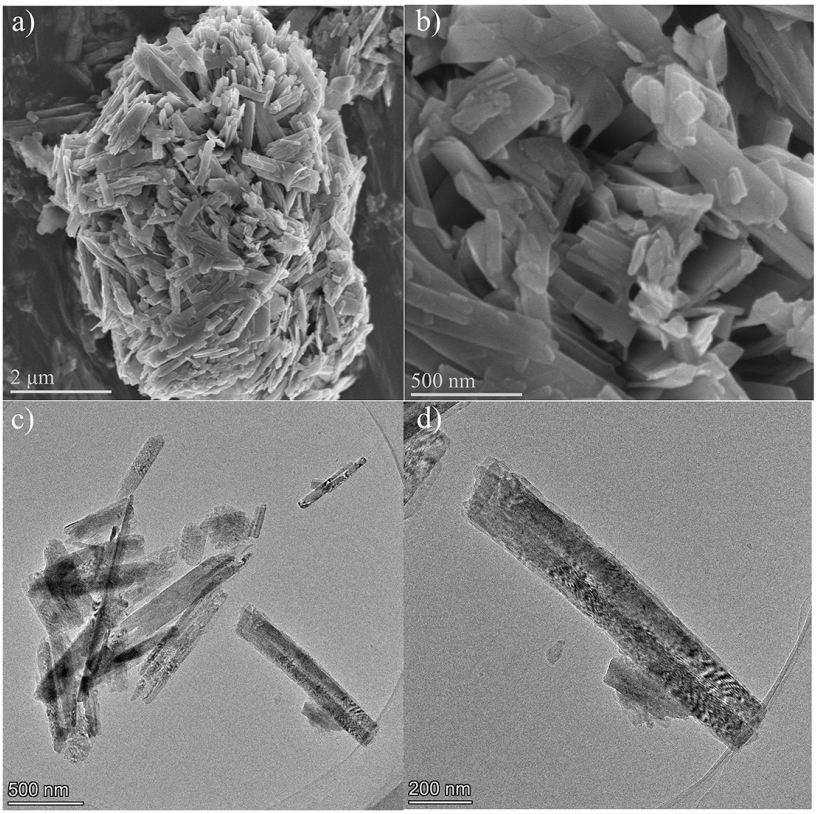

Fig. S4. (a, b) SEM and (c, d) TEM images of $VO_2 \cdot 0.26H_2O$.

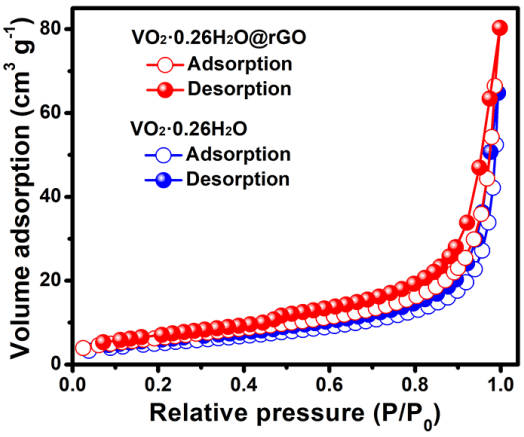

Fig. S5. Nitrogen adsorption-desorption isotherms.

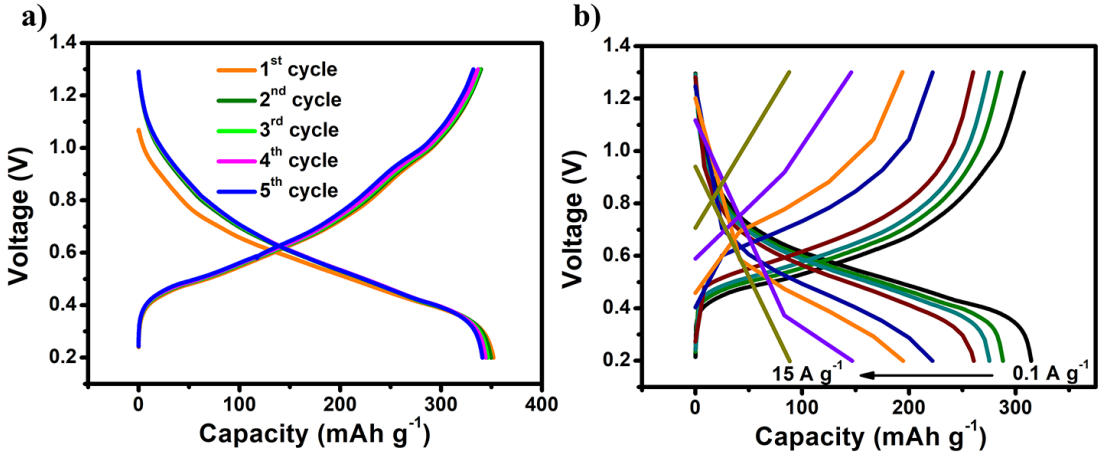

Fig. S6. (a) Galvanostatic charge-discharge curves at 0.1 A g^{-1} and (b) galvanostatic charge-discharge plots at different current densities of $VO_2 \cdot 0.26H_2O$.

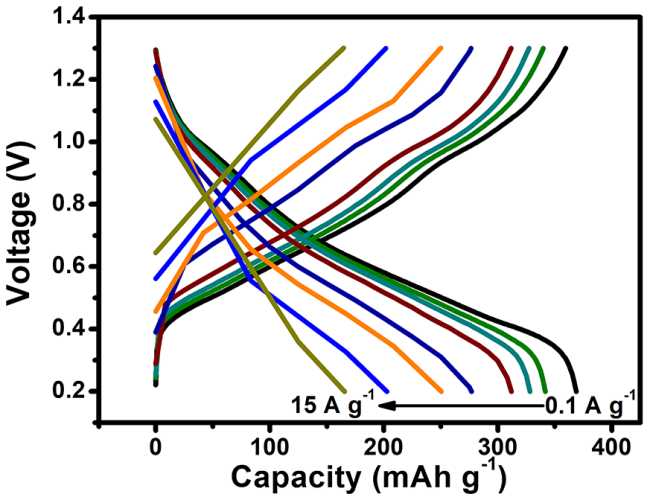

Fig. S7. Galvanostatic charge-discharge plots at different current densities of $VO_2 \cdot 0.26H_2O$@rGO.

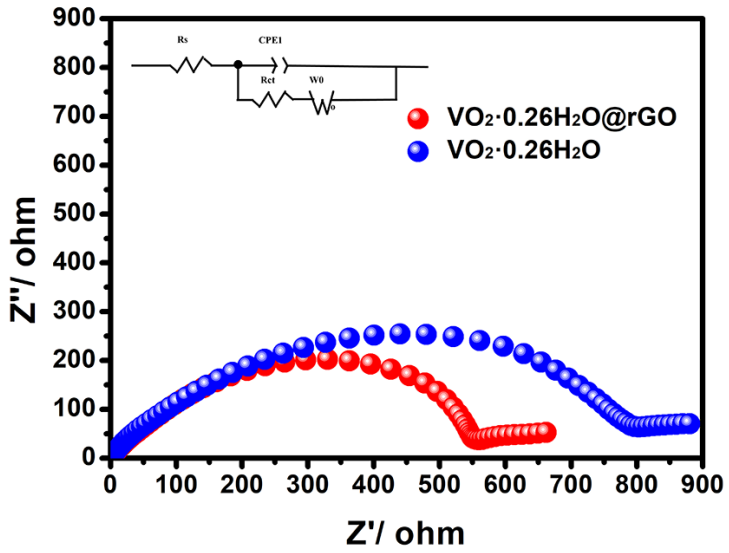

Fig. S8. EIS plots of $VO_2 \cdot 0.26H_2O$ and $VO_2 \cdot 0.26H_2O$@rGO.

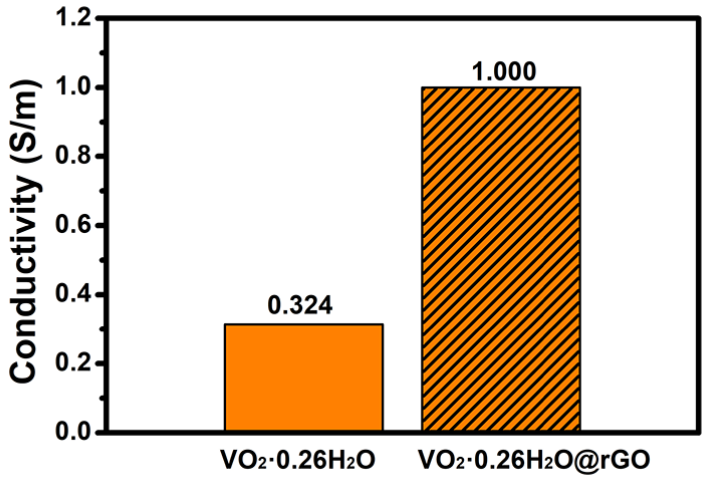

Fig. S9. Conductivity of $VO_2 \cdot 0.26H_2O$ and $VO_2 \cdot 0.26H_2O$@rGO.

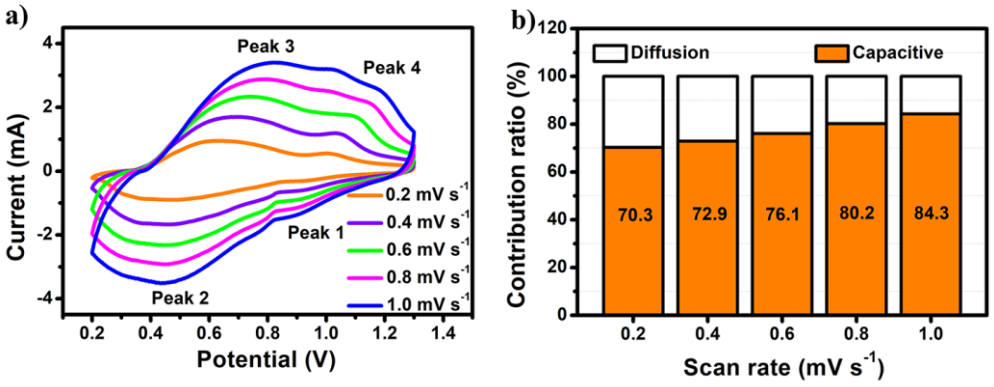

Fig. S10. (a) CV curves at different scan rates and (b) the capacitive contribution ratio at various scan rates of $VO_2 \cdot 0.26H_2O$.

In principle, the peak current (v) and scan rate (v) in CV curves obey the following formula:

$$i = av^b \quad (1)$$

where a and b are variable parameters, b represents the slope of log (i) vs. log (v) plot. Generally, the b value of 0.5 represents the electrode process is controlled by the ion diffusion process, and the b value of 1 demonstrates pseudocapacitance controls the electrode process.

The contribution ratio of the pseudocapacitive effect can be determined by the following equations: [5,6]

$$i(V) = k_1 v + k_2 v^{1/2} \quad (2)$$

And this can be reformulated as:

$$i/v^{1/2} = k_1 v^{1/2} + k_2 \quad (3)$$

where i, $k_1 v$, and $k_2 v^{1/2}$ represent the current, capacitive contribution, and Faradaic intercalation effect, respectively.[7,8]

The values of k1 and k2 are obtained by fitting the formula (3).

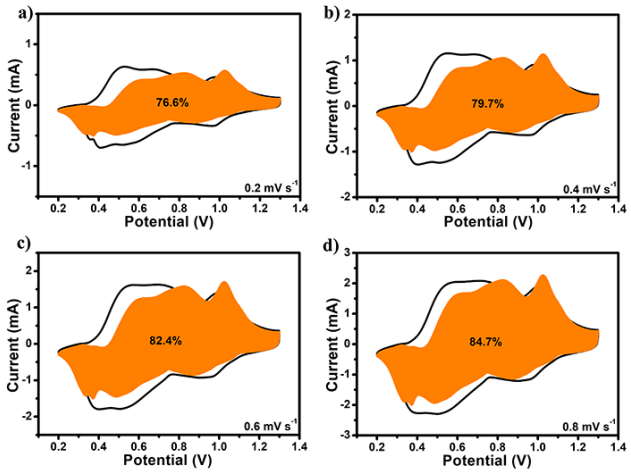

Fig. S11. CV curves with capacity separation of $VO_2 \cdot 0.26H_2O$@rGO.

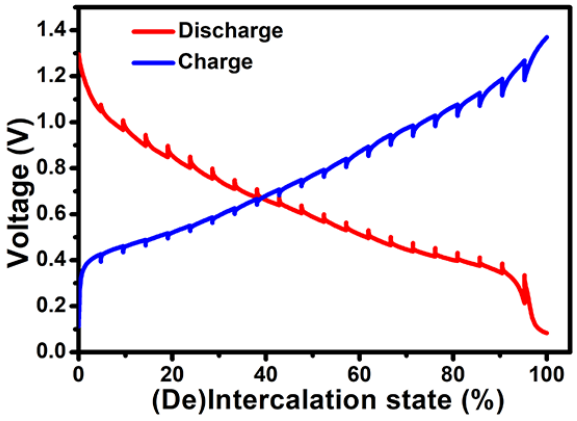

Fig. S12. GITT curves at 0.1 A g^{-1} for $VO_2 \cdot 0.26H_2O$.

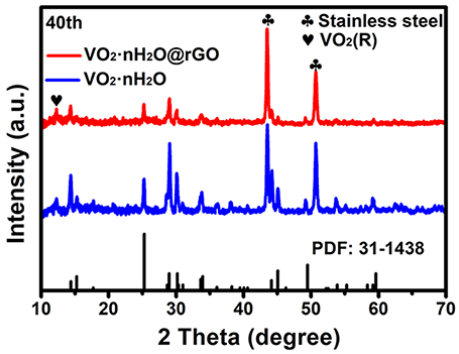

Fig. S13. XRD patterns after 40 cycles of $VO_2 \cdot 0.26H_2O$ and $VO_2 \cdot 0.26H_2O$@rGO electrodes.

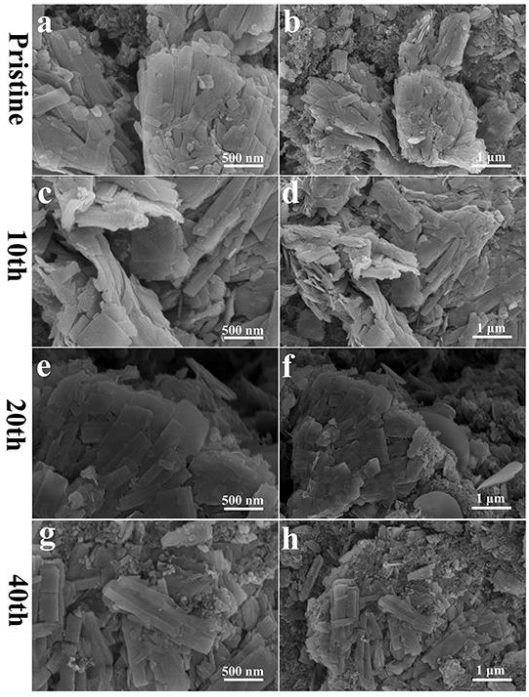

Fig. S14. SEM images of $VO_2 \cdot 0.26H_2O$@rGO electrodes for (a, b) pristine state, (c, d) 10^{th} cycle, (e, f) 20^{th} cycle, (g, h) 40^{th} cycle.

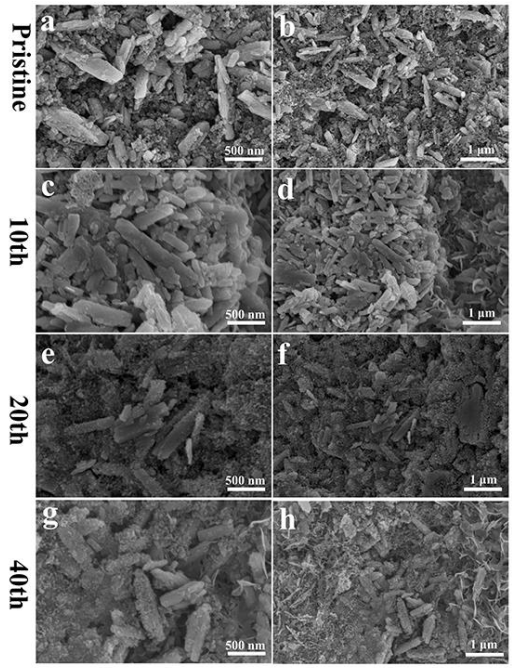

Fig. S15. SEM images of $VO_2 \cdot 0.26H_2O$ electrodes for (a, b) pristine state, (c, d) 10^{th} cycle, (e, f) 20^{th} cycle, (g, h) 40^{th} cycle.

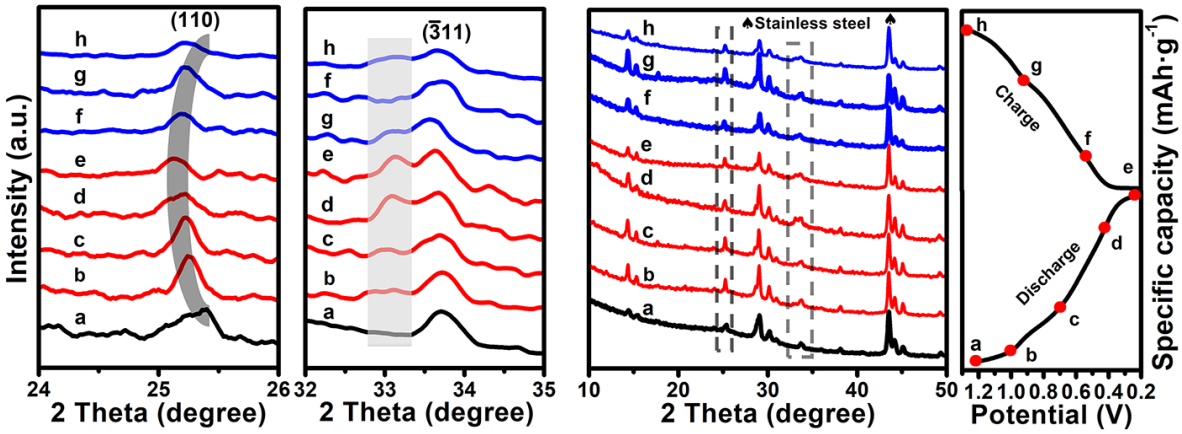

Fig. S16. Ex-situ XRD patterns of $VO_2 \cdot 0.26H_2O$.

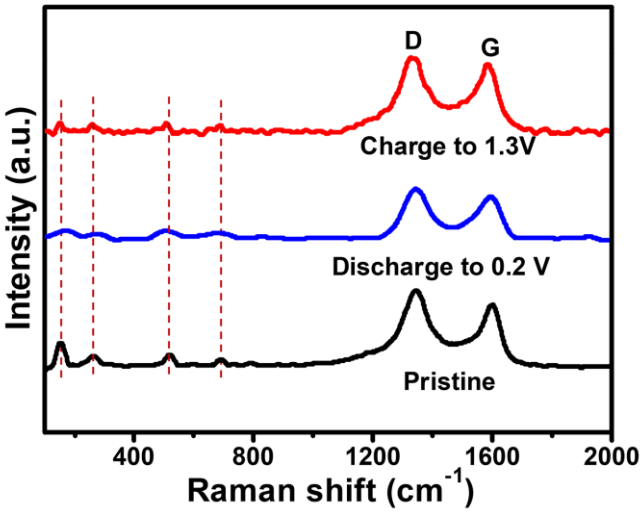

Fig. S17. Ex situ Raman patterns of $VO_2 \cdot 0.26H_2O$@rGO.

References

1 D. Jia, K. Zheng, M. Song, H. Tan, A. Zhang, L. Wang, L. Yue, D. Li, C. Li and J. Liu, *Nano Res.*, 2020, **13**, 215-224.

2 Y. Liu, and X. Wu, *Nano Energy*, 2021, **86**, 106124.

3 F. Cui, J. Zhao, D. Zhang, Y. Fang, F. Hu and K. Zhu, *Chem. Eng. J.*, 2020, **390**, 124118.

4 X. Hu, Z. Zhao, L. Wang, J. Li, C. Wang, Y. Zhao and H. Jin, *Electrochim. Acta*, 2019, **293**, 97-104.

5 T. Brezesinski, J. Wang, S.H. Tolbert and B. Dunn, *Nat. Mater.*, 2010, **9**, 146, 151.

6 J. Wang, J. Polleux, J. Lim and B. Dunn, *J. Phys. Chem. C*, 2007, **111**, 14925-14931.

7 P. Simon, Y. Gogotsi and B. Dunn, *Science*, 2014, **343**, 1210-1211.

8 K. Zhang, Z. Hu, X. Liu, Z. Tao and J. Chen, *Adv. Mater.*, 2015, **27**, 3305-3309.